

# Obesity-induced miR-802 directly targets AMPK and promotes nonalcoholic steatohepatitis in mice



Hao Sun, Sunmi Seok, Hyunkyung Jung, Byron Kemper, Jongsook Kim Kemper\*

## ABSTRACT

**Objective:** Obesity-associated nonalcoholic fatty liver disease (NAFLD) is a leading cause of liver failure and death. However, the pathogenesis of NAFLD and its severe form, nonalcoholic steatohepatitis (NASH), is poorly understood. The energy sensor, AMP-activated protein kinase (AMPK), has decreased activity in obesity and NAFLD, but the mechanisms are unclear. Here, we examined whether obesity-induced miR-802 has a role in promoting NASH by targeting AMPK. We also investigated whether miR-802 and AMPK have roles in modulating beneficial therapeutic effects mediated by obeticholic acid (OCA), a promising clinical agent for NASH.

**Methods:** Immunoblotting, luciferase assays, and RNA-protein interaction studies were performed to test whether miR-802 directly targets AMPK. The roles of miR-802 and AMPK in NASH were examined in mice fed a NASH-promoting diet.

**Results:** Hepatic miR-802 and AMPK levels were inversely correlated in both NAFLD patients and obese mice. MicroRNA *in silico* analysis, together with biochemical studies in hepatic cells, suggested that miR-802 inhibits hepatic expression of AMPK by binding to the 3' untranslated regions of both human *AMPK $\alpha$ 1* and mouse *Ampk $\beta$ 1*. In diet-induced NASH mice, OCA treatment reduced hepatic miR-802 levels and improved AMPK activity, ameliorating steatosis, inflammation, and apoptosis, but these OCA-mediated beneficial effects on NASH pathologies, particularly reducing apoptosis, were reversed by overexpression of miR-802 or downregulation of AMPK.

**Conclusions:** These results indicate that miR-802 inhibits AMPK by directly targeting *Ampk $\beta$ 1*, promoting NAFLD/NASH in mice. The miR-802-AMPK axis that modulates OCA-mediated beneficial effects on NASH may represent a new therapeutic target.

© 2022 The Author(s). Published by Elsevier GmbH. This is an open access article under the CC BY-NC-ND license (<http://creativecommons.org/licenses/by-nc-nd/4.0/>).

**Keywords** NAFLD; NASH; OCA; FXR; Inflammation; Hepatocellular apoptosis

## 1. INTRODUCTION

Nonalcoholic fatty liver disease (NAFLD) is the most common chronic liver disease and a leading cause of liver-related death [1,2]. As a hepatic manifestation of obesity-related metabolic syndrome, NAFLD is highly associated with type 2 diabetes, dyslipidemia, and cardiovascular disease. NAFLD begins with simple steatosis but may progress to its more severe form, nonalcoholic steatohepatitis (NASH) and later, fatal cirrhosis and hepatocellular carcinoma [1,2]. Despite the striking increase in global prevalence of NAFLD, the underlying mechanisms of the pathogenesis of NAFLD are poorly understood and treatment options are limited.

MicroRNAs (miRs) are negative gene regulators that have great therapeutic potential for many diseases, including the NAFLD [3]. Expression of miRs is often aberrantly up- or down-regulated in human disease, including obesity and NAFLD [3]. For instance, obesity-induced miR-34a inhibits multiple targets in energy metabolism, such as SIRT1,  $\beta$ -Klotho, PPAR $\alpha$ , and HNF-4 $\alpha$ , promoting fatty liver and insulin resistance [4–9]. Further, miR-802 in obesity impairs glucose regulation by targeting HNF1 $\beta$  [10] and inhibits insulin

production by targeting NeuroD [11]. The mechanisms for aberrant expression of miRs in obesity are generally understudied, but aberrant activation of the gene-regulatory proteins, CRTC2 and FOXO1, was shown to increase transcription of hepatic *miR-34a* and *pancreatic miR-802*, respectively [11–14]. Further, defective nuclear receptor FXR-SHP function increased hepatic expression of *miR-34a* and *miR-802* in obesity [4,15]. Indeed, treatment with obeticholic acid (OCA), an FXR agonist currently in clinical trials for NASH [16], decreased hepatic miR-802 levels, ameliorating insulin resistance and fatty liver in mice [15], but the role of miR-802 in NASH has not been determined.

AMP-activated protein kinase (AMPK) is a master energy sensor that plays a key role in energy metabolism [17–19]. Under low energy conditions, AMPK is activated and thus, increases cellular energy levels by inhibiting biosynthetic pathways and activating catabolic pathways [20–22]. For instance, AMPK decreases hepatic triglyceride (TG) levels by inhibiting lipogenesis and promoting fatty acid  $\beta$ -oxidation. Since the activity of AMPK is reduced in obesity and NAFLD [17,18,23], increasing AMPK activity has been suggested as an attractive therapeutic option for metabolic diseases, including NAFLD. Indeed, pharmacological activation of AMPK prevented NAFLD [24] and

Department of Molecular and Integrative Physiology, University of Illinois at Urbana-Champaign, Urbana, IL, 61801, USA

\*Corresponding author. Department of Molecular and Integrative Physiology, University of Illinois at Urbana-Champaign, 407 S. Goodwin Avenue, Urbana, IL, 61801, USA  
E-mail: [jongsook@illinois.edu](mailto:jongsook@illinois.edu) (J.K. Kemper).

Received September 5, 2022 • Accepted September 13, 2022 • Available online 17 September 2022

<https://doi.org/10.1016/j.molmet.2022.101603>

**List of Abbreviations**

ACC	acetyl coA carboxylase
AGO2	Argonaute2
AMPK	AMP-activated protein kinase
ALT	alanine aminotransferase
ALP	alkaline phosphatase
CHX	cycloheximide
FASN	fatty acid synthase
FXR	Farnesoid-X-Receptor
miR	microRNA
HFCF	high fat cholesterol and fructose
H&E	hematoxylin and eosin
HMGCR	HMG-CoA reductase

IB	immunoblotting
IHC	immunohistochemistry
NAFLD	nonalcoholic fatty liver disease
NASH	nonalcoholic steatohepatitis
OCA	obeticholic acid
ORO	oil red o
RIP	RNA-binding protein immunoprecipitation
RISC	RNA-induced silencing complex
ROR $\alpha$	RAR-related orphan receptor $\alpha$
SHP	Small Heterodimer Partner
SIRT1	Sirtuin1
TG	triglyceride
TUNEL	terminal deoxynucleotidyl transferase dUTP nick end labeling
3' UTR	3' untranslated region

liver-specific activation of AMPK protected against NAFLD/NASH in mice [20,21]. While reactivation of AMPK in NAFLD improved hepatic steatosis, complete knockout of hepatic AMPK did not promote fatty liver development [25]. Although AMPK has received great attention as a promising therapeutic target for metabolic disease, the mechanisms underlying the low activity of AMPK in obesity and NAFLD are not fully understood.

In this study, we show that obesity-induced miR-802 inhibits expression and activity of AMPK, which contributes to NAFLD/NASH. In mice fed a NASH-promoting diet, we also show that the miR-802-AMPK axis can modulate OCA-mediated beneficial effects on NASH pathologies, particularly reducing hepatocellular apoptosis.

## 2. MATERIALS AND METHODS

### 2.1. Animal experiments

Mice were housed at 23 °C with 50% humidity under a 12 h/12 h light/dark cycle, and food and water were available ad libitum. For evaluating the roles of miR-802 and AMPK in NASH, C57BL/6 male mice were fed a high fat/cholesterol/fructose diet (Research Diets, D09100310, 40 kcal% fat, 2% cholesterol, 20 kcal% fructose), termed the Amylin liver NASH (AMLN) diet, for 7–9 weeks to promote NASH [1,26]. Then, the mice were injected with 100  $\mu$ l of 0.5–1  $\times$  10<sup>9</sup> active viral particles of adenovirus expressing miR-802-5p, shRNA for *Ampk $\alpha$ 1*, or control GFP, and were treated with vehicle or a low dose of OCA (3 mg/kg/day, in 1% methylcellulose) by oral gavage daily for 2 weeks. Injection of these adenoviral doses does not elicit marked inflammatory responses [27–29]. For miR-802 downregulation studies, mice were fed a high fat diet (HFD) (Envigo Teklad, TD88137) for 15 weeks and then were injected with adenovirus expressing antisense-miR-802 or control GFP for 1 week. For miR-802 overexpression studies, mice fed normal chow were injected with adenovirus expressing miR-802-5p or control GFP for 1 week.

### 2.2. Study approval

Animal protocols were approved by the Institutional Animal Care and Use Committee, experiments were approved by the Institutional Biosafety Committee, and all experiments were performed in accord with the ethical guidelines of the National Institutes of Health (NIH).

### 2.3. Human NAFLD patients

Liver specimens from normal individuals without liver disease or NAFLD steatosis patients were obtained from the Liver Tissue Cell Procurement and Distribution System that operates under a contract

from the NIH. Because no one on our study team has access to the subject identifiers linked to the specimens or data, this study is not considered human research and ethical approval was not required.

### 2.4. Histological analyses

Liver tissue was frozen in OCT compound (Sakura Finetek, 4583), sectioned, and stained with H&E or with Oil Red-O. Paraffin-embedded liver sections were incubated with F4/80 antibody, and antibody was detected using a peroxidase-based method (ab64238, Abcam). Liver collagen was detected by Sirius Red staining (Abcam, ab246832) and apoptosis was detected by TUNEL staining (Millipore, S7100). Liver sections were imaged with a NanoZoomer Scanner (Hamamatsu) and quantification was done using NIH ImageJ.

### 2.5. Immunoblotting (IB)

Liver tissues were washed with ice-cold PBS and homogenized in RIPA buffer (50 mM Tris-HCl, pH 7.5, 1 mM EDTA, 0.5% NP40, 1% sodium deoxycholate, 1 mM DTT, 0.5% SDS, 0.2 mM PMSF, 1  $\mu$ g/ml pepstatin, 0.5  $\mu$ g/ml leupeptin, 5 mM NaF, and 2 mM Na<sub>3</sub>VO<sub>4</sub>) and then, sonicated briefly for 3–5 s to prepare liver lysates for IB analyses. Band densities were quantified using the NIH ImageJ program. Protein levels of p-AMPK at Thr-172 and p-ACC at Ser-79 were determined by IB and those of p-HMGCR and p-FXR at Ser residues, phosphorylation targets of AMPK [30,31], were measured by IP followed by IB using a pan p-Ser antibody. Information on antibodies is provided in Supplementary Information.

### 2.6. Measurement of AMPK activity in hepatocytes

Primary mouse hepatocytes (PMH) were isolated as described previously [15,32–34]. Isolated hepatocytes were transfected with 5–50 nM pre-miR-802, antisense-miR-802, or siRNA for *Ampk $\beta$ 1* (ON-TARGETplus SMART pool, Dharmacon), and 2 days later, cells were harvested. For miR-802 downregulation, 24 h after transfection, cells were treated with palmitic acid (300  $\mu$ M) for 24 h and harvested. AMPK activity was determined by an HRP-conjugated ELISA (BioAssay Systems, EAMPK-100).

### 2.7. Measurement of levels of liver TG/cholesterol and plasma ALP/ALT

Hepatic levels of TG and cholesterol (Sigma TR0100 and Sigma MAK043, respectively) and plasma levels of ALP and ALT (Abcam ab83369 and Sigma MAK052, respectively) were determined according to the manufacturer's instructions.

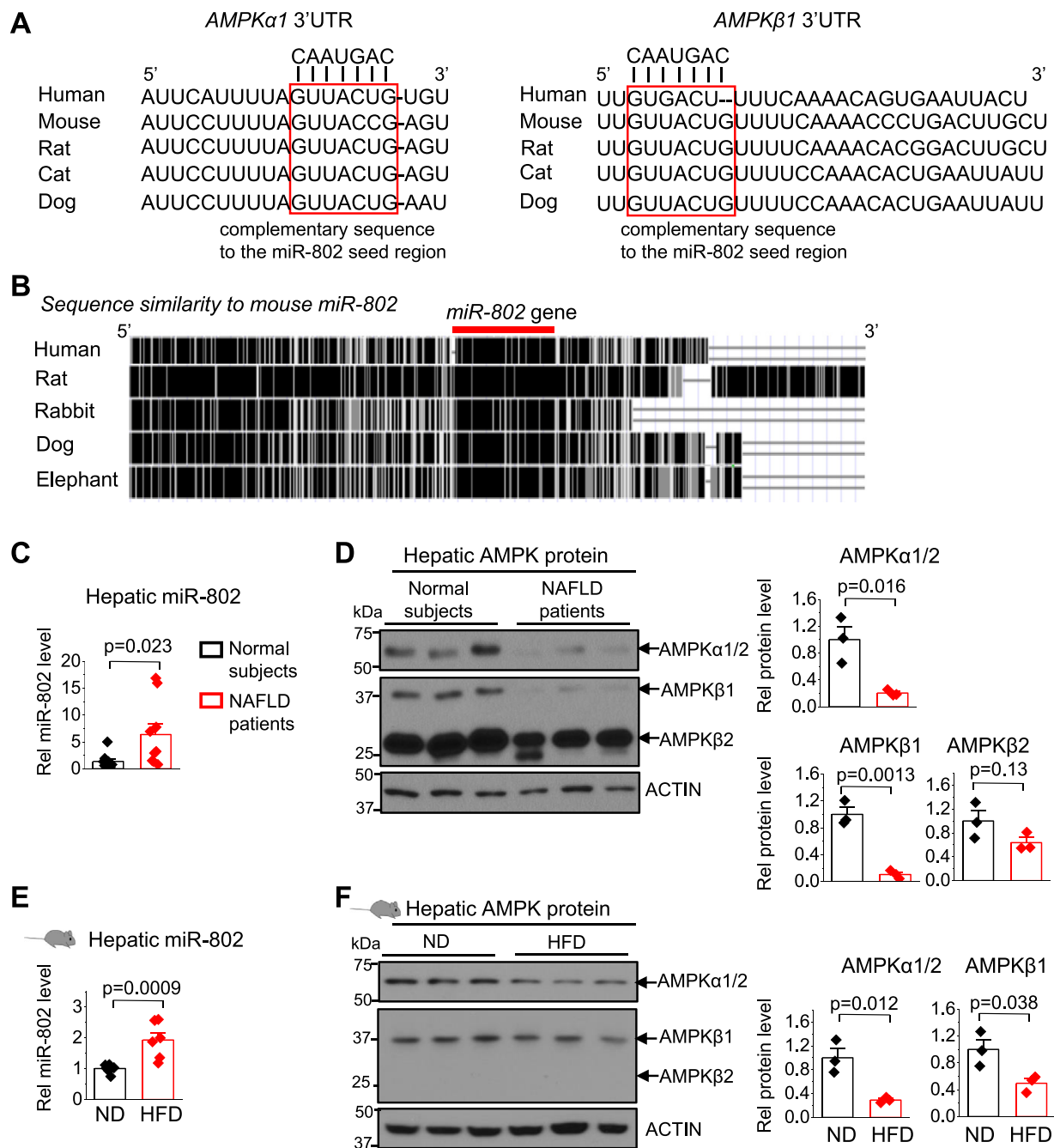


**Figure 1: Hepatic levels of miR-802 and AMPK are inversely correlated in both NAFLD patients and dietary obese mice.** (A) Comparison of mammalian 3'UTRs of *AMPK $\alpha$ 1* (left) and *AMPK $\beta$ 1* (right) mRNAs that contain complementary sequences (boxed) to the seed region of miR-802 (CAAUGAC). (B) Similarity of mammal sequences aligned to 2.5 kb of mouse sequence containing the miR-802 gene. Black vertical bars indicate bp identical to the mouse sequence and the position of the conserved miR-802 gene is indicated. (C) Hepatic miR-802 levels in liver lysates from normal subjects (n = 10) and NAFLD patients (n = 9). (D) Liver extracts from 9 normal or NAFLD patients were randomly combined to form 3 pooled samples/lane. Levels of the indicated proteins detected by IB (left) and quantitation using Image J (right). (E–F) C57BL/6 mice (n = 3 mice) were fed a normal chow diet (ND) or a high fat diet (HFD) for 12 weeks. (E) Hepatic miR-802 levels (n = 6). (F) Levels of the indicated proteins detected by IB (left) and quantitation using Image J of AMPK protein bands relative to actin (right, n = 3 mice). (C–F) The mean and standard error of the mean (SEM) are plotted. Statistical significance was determined by the Student's t-test. P values are indicated.

## 2.8. RT-qPCR

Levels of miRNAs were determined using TaqMan™ MicroRNA Assay (ThermoFisher, 4427975) and normalized to SnoRNA. Levels of mRNAs were measured by RT-qPCR using primers listed in Supplemental Table 1 and normalized to 36B4 mRNA.

## 2.9. Luciferase reporter assays

The 3' UTR regions harboring the miR-802 binding site of human *AMPK $\alpha$ 1* (310 bp, +2569/+2878) and mouse *Ampk $\beta$ 1* (249 bp, +801/+1059) were amplified from genomic DNA isolated from human HepG2 (ATCC, HB-8065) and mouse Hepa1c1c7 (ATCC,

CRL-2026) cells, respectively. The amplified fragments were inserted into pmirGLO luciferase reporter (Promega, E1330) and mutations were introduced in the miR-802 site by site-directed mutagenesis (Agilent, 200521). Cells were transfected with 200 ng of luciferase reporter plasmids, 200 ng of  $\beta$ -galactosidase plasmid, and 1–50 nM precursor-miR-802, and harvested 2 days later. The values for luciferase activities were normalized to  $\beta$ -galactosidase activities.

### 2.10. Cycloheximide (CHX) study

Protein stability studies using CHX were done as previously described [35–37]. Briefly, Hepa1c1c7 cells were transfected with 50 nM siRNA for AMPK $\beta$ 1, and 2 days later, cells were treated with 10  $\mu$ g/ml CHX for the indicated times. AMPK $\alpha$  protein levels in cell lysates were detected by IB.

### 2.11. RNA-binding protein immunoprecipitation (RIP)

Hepa1c1c7 cells were transfected with 1 nM pre-miR-802, and 24 h later, cells were lysed in RIPA buffer with 0.5 mM DTT, protease inhibitors and 250 unit/ml RNase inhibitor (Promega, N2515). Cell lysates were incubated with 1  $\mu$ g AGO2 antibody at 4 °C for 1 h and then, incubated with protein G Sepharose beads for 1 h. The beads were washed 4 times with RIPA buffer containing 1 M NaCl, and then, incubated with Proteinase K at 45 °C for 15 min. RNAs were recovered using miRNeasy (Qiagen, ID 217004) and levels of RNAs were determined by RT-qPCR using primers listed in Supplemental Table 2.

### 2.12. Statistical analysis

OriginPro 2020b was used for data analysis. Statistical analysis of different groups was performed using the Student's unpaired t-test or one-way ANOVA with Tukey post-test as appropriate. The mean and standard errors (SEM) are presented and differences with  $p < 0.05$  were considered statistically significant.

## 3. RESULTS

### 3.1. Elevated miR-802 levels in both NAFLD patients and obese mice correlate with decreased protein AMPK levels

The activity of the AMPK heterotrimer complex is repressed in obesity and NAFLD [17–19,23], but the underlying mechanisms are not clearly understood. Complementary sequences to the miR-802 seed region (CAAUGAC) are conserved in the 3'untranslated regions (3'UTRs) of one or both AMPK $\alpha$ 1 and AMPK $\beta$ 1 mRNAs in mammals (Figure 1A) and *miR-802* gene sequences are also highly conserved (Figure 1B). Since the AMPK complex is obligate for its catalytic function [17,22], inhibition of the expression of either  $\alpha$  or  $\beta$  subunit by miR-802 results in the same outcome of decreased AMPK activity. We, therefore, hypothesized that obesity-induced miR-802 promotes NAFLD by directly targeting AMPK.

We first examined expression of miR-802 and AMPK in liver samples of NAFLD steatosis patients and in diet-induced obese mice. Compared to normal individuals, hepatic miR-802 levels are elevated in the NAFLD patients (Figure 1C) and protein levels of AMPK $\alpha$ 1/2 and  $\beta$ 1 were substantially reduced, over 80%, while  $\beta$ 2 levels were modestly reduced in the patients (Figure 1D). In dietary obese mice, hepatic miR-802 levels were also elevated (Figure 1E), and conversely, protein levels of AMPK $\alpha$ 1/2 and  $\beta$ 1 were reduced, compared to mice fed normal chow (Figure 1F). These results show a strong inverse correlation between hepatic expression of miR-802 and AMPK in both NAFLD patients and obese mice.

### 3.2. MiR-802 binds to the 3'UTRs of both mouse *Ampk $\beta$ 1* and human *AMPK $\alpha$ 1*

We next determined if the predicted miR-802 binding sites in the 3'UTR sequences of mouse *Ampk $\beta$ 1* and human *AMPK $\alpha$ 1* mRNAs (Figure 1A) are functional. The 3' UTRs of both mouse *Ampk $\beta$ 1* and human *AMPK $\alpha$ 1* mRNAs containing the wild type (WT) miR-802 recognition sequence, or a mutated sequence, were inserted into a luciferase reporter, and reporter assays were performed in primary mouse hepatocytes and human HepG2 cells, respectively.

Overexpression of miR-802 modestly, but significantly, inhibited the activity of luciferase reporters containing the WT sequence but not the mutated sequence in mouse hepatocytes (Figure 2A). Similarly, in human HepG2 cells, overexpression of miR-802 significantly inhibited the activity of luciferase reporters containing the WT miR-802 sequence from the 3' UTR of human *AMPK $\alpha$ 1* mRNA, but not the mutated sequence (Figure 2B). These results suggest that miR-802 binds to the 3'UTRs of both mouse *Ampk $\beta$ 1* and human *AMPK $\alpha$ 1* mRNAs.

### 3.3. Association of miR-802 and 3'UTR of *Ampk $\beta$ 1* with the AGO2 complex

MiRs inhibit protein translation and/or promote mRNA degradation by guiding the argonaute2 (AGO2)-containing RNA-induced silencing complex (RISC) to the 3'UTR of target mRNAs [38]. To test whether miR-802 and the 3'UTR of *Ampk $\beta$ 1* associate with the AGO2-RISC complex, we performed RNA-binding protein immunoprecipitation (RIP) assays in Hepa1c1c7 cells (Figure 2C). Cytosolic mature miR-802 sequences were significantly enriched in the AGO2 complex, but the nuclear primary miR-802 (pri-miR-802) sequences were not detectable (Figure 2D). Further, the 3'UTR of *Ampk $\beta$ 1* mRNA was enriched in the complex while the 3'UTR of control *Actin* mRNA was not (Figure 2E). These results suggest that miR-802 and the 3'UTR of *Ampk $\beta$ 1* mRNA are associated with the AGO2 complex (Figure 2F) and further supports the conclusion that miR-802 binds to the 3'UTRs of *Ampk $\beta$ 1* mRNA resulting in gene silencing.

### 3.4. Overexpression of miR-802 decreases, whereas downregulation of miR-802 increases, AMPK expression and activity in hepatocytes

Since hepatic miR-802 and AMPK levels are inversely correlated in obese mice (Figure 1E,F), we next tested whether the modulation of miR-802 levels by its overexpression or downregulation affects expression of AMPK $\beta$ 1 and AMPK activity in primary mouse hepatocytes (PMH).

Overexpression of precursor miR-802 resulted in decreases in both *Ampk $\beta$ 1* mRNA levels and AMPK activity in a dose-dependent manner (Figure 3A). Conversely, in hepatocytes treated with palmitate to mimic obesity, antisense oligonucleotide-mediated downregulation of miR-802 resulted in increases in both *Ampk $\beta$ 1* mRNA levels and AMPK activity (Figure 3B). Protein levels of p-AMPK $\alpha$  phosphorylated at Thr-172, an indicator of the AMPK activity [17,18,22], were increased after miR-802 downregulation (Figure 3C). The inverse correlations between miR-802 and AMPK expression/activity, together with biochemical studies in hepatic cells (Figure 2), suggest that miR-802 directly targets AMPK, reducing hepatic AMPK function.

### 3.5. The AMPK $\beta$ subunit is important for stability of the AMPK $\alpha$ subunit

The heterodimer complex of AMPK is obligate for its catalytic function [17,22]. The overexpression of miR-802 decreased both expression of the AMPK $\beta$ 1 subunit and the activity of AMPK in mouse hepatocytes (Figure 3A) whereas downregulation of miR-802 had the opposite effect



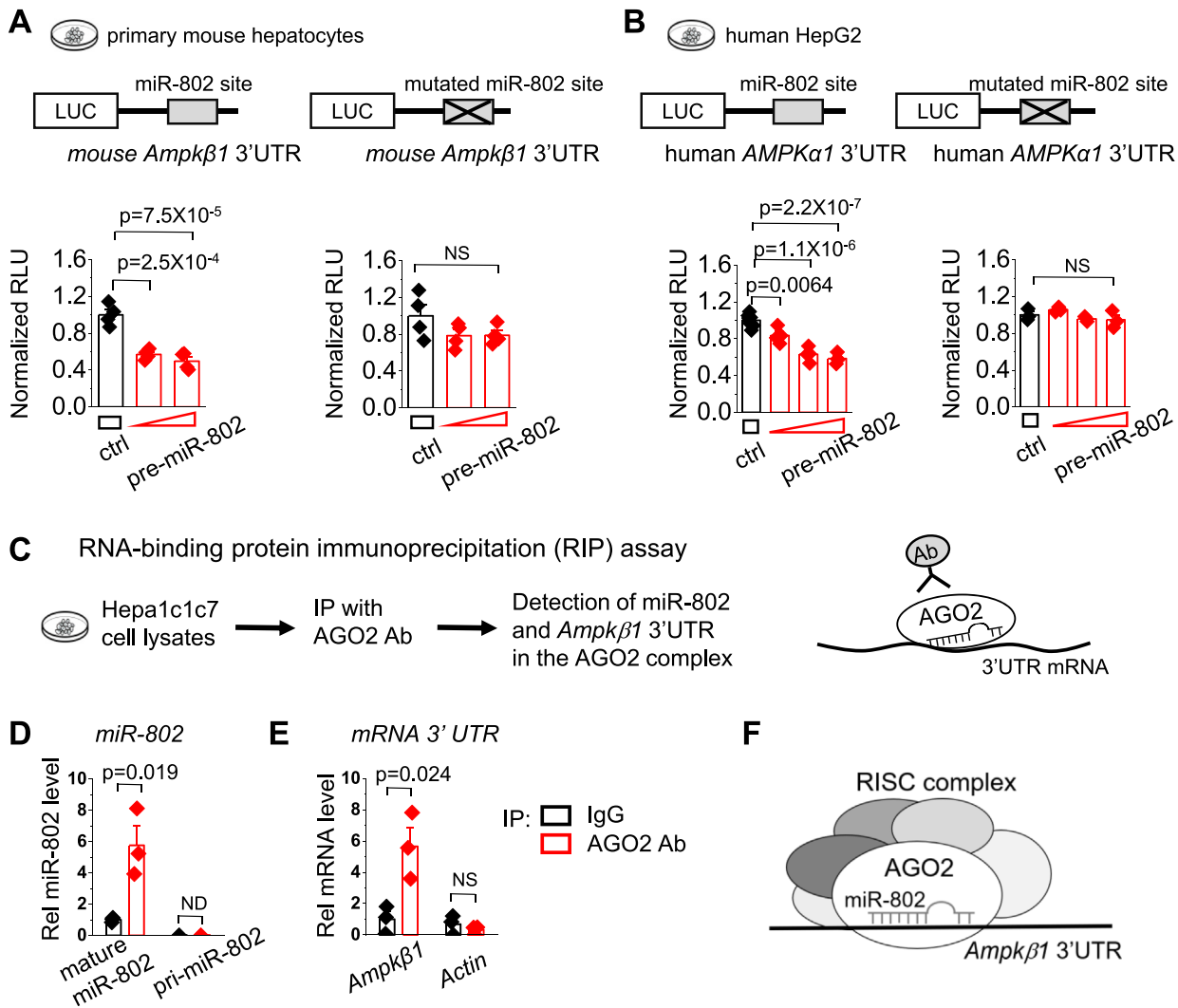


**Figure 2:** (A–D) MiR-802 binds to the 3'UTR of mouse *Ampkβ1* and human *AMPKα1*. (A, B) The 3' UTR sequences of mouse *Ampkβ1* (A) or human *Ampkα1* (B) mRNAs containing either the wild type miR-802 binding site or a mutated site were inserted 3' of the luciferase gene in a reporter vector (top). Primary mouse hepatocytes (A) or human HepG2 (B) cells were transfected with control RNA (ctrl) or pre-mouse-miR-802 or pre-human-miR-802, respectively, together with either wild type (left) or mutated (right) luciferase vectors for 48 h. Luciferase activity in cell extracts normalized to β-galactosidase activity (n = 4–8 wells in 3 (A) and 2 (B) independent experiments). (C–E) Association of the 3'UTR of *Ampkβ1* and miR-802 with the AGO2 complex. (E) Experimental scheme: Hepa1c1c7 cells were transfected with pre-miR-802 for 1 day and cell lysates were incubated with IgG or antibody to AGO2, a component of the RISC complex. Levels of mature miR-802 or pre-miR-802 (D) and 3'UTRs of *Ampkβ1* or actin mRNAs (E) in the immunoprecipitates were determined by RT-qPCR (n = 3). (F) Model of miR-802 bound to the 3'UTR of *Ampkβ1* mRNA in the AGO2-containing RISC complex. (A,B,D,E) The mean and SEM are plotted. Statistical significance was determined by the one-way ANOVA (A,B) or by the Student's t-test (D,E). P values are indicated. ND, not detectable. NS, not significant.

(Figure 3B). Downregulation also results in increased protein levels of p-AMPKα and AMPKα (Figure 3C). To test whether the reduced AMPKβ1 levels and consequently, reduced AMPK complex levels results in increased degradation of the AMPKα subunit and subsequently, AMPK activity, AMPKβ1 was downregulated in Hepa1c1c7 cells by siRNA. Downregulation of AMPKβ1 substantially reduced protein levels of the AMPKα subunit (Figure 3D), suggesting that stability of the α subunit is dependent on incorporation into the complex.

To further test whether the reduced β1 levels lead to decreased protein stability of the α subunit, we examined the effect of downregulation of AMPKβ1 on the protein degradation of AMPKα by inhibiting protein synthesis with cycloheximide (CHX) and measuring AMPKα protein levels over time. The AMPKα subunit was relatively

stable in Hepa1c1c7 cells, with little decrease of protein levels even after 9 h of CHX treatment (Figure 3E). In contrast, downregulation of AMPKβ1 substantially decreased AMPKα levels at the initiation of CHX treatment, and progressively reduced levels to about 50% of the initial level after 9 h of CHX treatment (Figure 3E). These results suggest that reduced levels of AMPKβ1 result in destabilization of AMPKα, possibly because the AMPKα is not incorporated into a stable complex.

### 3.6. Downregulation of miR-802 in dietary obese mice improves AMPK activity

MiR-802 levels are increased in obesity [10,11,15], where hepatic AMPK activity is low [23,26]. We, thus, examined whether the miR-802

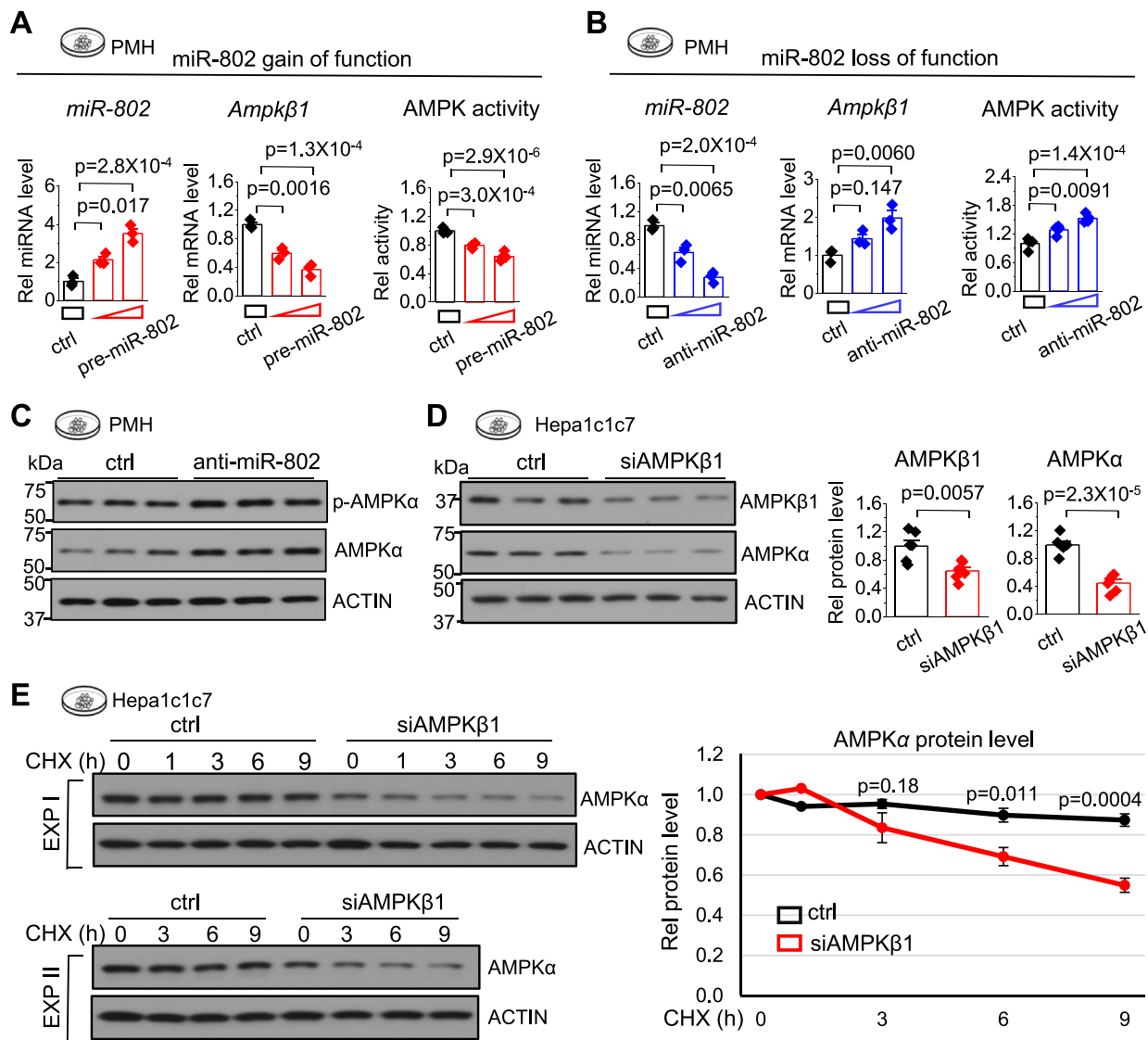


**Figure 3: (A–D) In PMH, overexpression of miR-802 decreases and downregulation of miR-802 increases AMPK levels and activity.** (A, B) Primary mouse hepatocytes (PMHs) were transfected with (A) control RNA (ctrl) or 5 or 50 nM of pre-miR-802 or (B) control RNA (ctrl) and 5 or 50 nM anti-miR-802 for 48 h. Levels of miR-802 and *Ampkβ1* mRNA levels were determined by RT-qPCR and AMPK activities were measured as described in the Experimental Procedures. (C) PMHs were transfected with control RNA (ctrl) or anti-miR-802 and 48 h later, treated with 300 μM palmitic acid (PA) for 24 h. The indicated proteins detected by IB (n = 3 culture dishes). (D) Hepa1c1c7 cells were transfected with control RNA (ctrl) or siRNA for *Ampkβ1* for 48 h. The indicated proteins in cell extracts detected by IB (left) and bands quantitated using Image J (right). **(E) Downregulation of AMPKβ1 reduces protein stability of the AMPKα1 subunit.** Mouse Hepa1c1c7 cells transfected with control RNA or siRNA of *Ampkβ1* for 48 h. Cells were then treated with 10 μg/ml cycloheximide (CHX) for the indicated times, and the indicated proteins in cells lysates were detected by IB. Two representative blots are shown (left) and quantitation of AMPKα levels normalized to actin with the 0-time level set to 1 is shown at the right (n = 3 culture dishes/time point). (A, B, D, E) The mean and SEM are plotted, and statistical significance was determined by the one-way ANOVA w/Tukey's test. P values are indicated.

has a role in decreased AMPK function in obesity. In diet-induced obese mice, hepatic levels of miR-802 were reduced by injection with adenovirus producing antisense-miR-802 (Figure 4A). Protein levels of AMPKβ1 in liver extracts were increased after miR-802 downregulation (Figure 4B). Protein levels of both p-AMPKα phosphorylated at Thr-172, an indicator of the AMPK activity [17,18,22], and AMPKα were also increased after miR-802 downregulation. Downregulation of miR-802 led to decreased neutral lipids and decreased hepatic TG levels (Figure 4C). These results indicate that

inhibition of miR-802 in obese mice improves AMPK function and hepatic steatosis.

### 3.7. Overexpression of miR-802 in lean mice reduces hepatic AMPK activity

Conversely, we tested whether overexpression of miR-802 in the liver of lean mice to the levels observed in obese mice (Figure 1E) can cause decreased AMPK activity. Adenoviral-mediated overexpression of miR-802 resulted in about a 2-fold increase in miR-802 levels (Figure 4D),

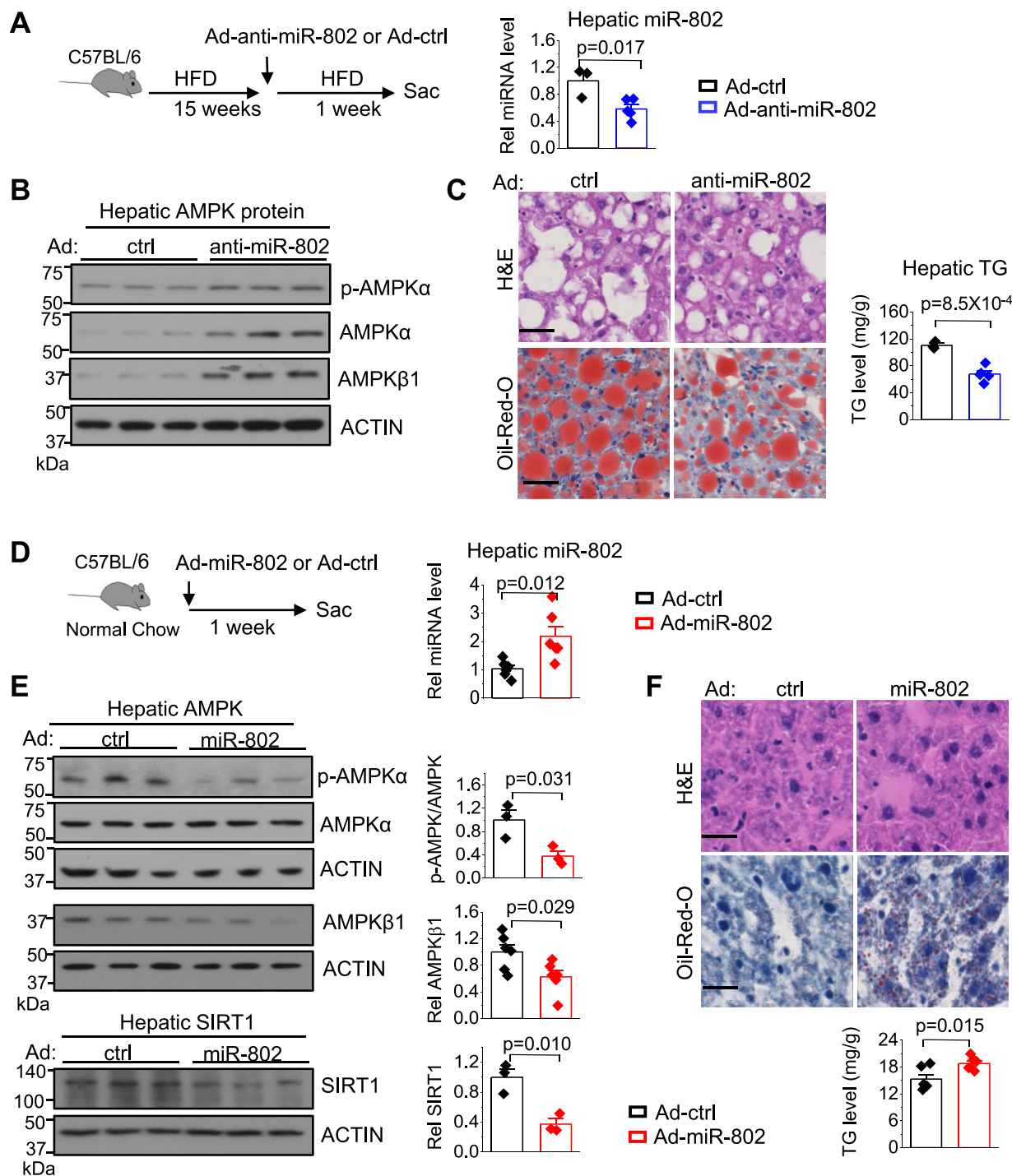


**Figure 4: (A–C) Downregulation of miR-802 in dietary obese mice increases AMPK expression and activity and decreases liver TG levels.** (A–C) To downregulate miR-802 expression, C57BL/6 mice were fed a HFD diet for 15 weeks, and then, injected via the tail vein with control adenovirus (Ad-ctrl) or adenovirus expressing antisense miR-802 one week before sacrifice. (A) Experimental scheme and hepatic miR-802 levels (right) ( $n = 3–5$  mice). (B) Protein levels of the indicated proteins in liver lysates determined by IB ( $n = 3$  mice). (C) H&E and Oil Red O staining of liver sections (left) and hepatic TG levels (right). (D–F) Conversely, overexpression of miR-802 in mice fed a normal chow decreases AMPK activity and increases liver TGs. C57BL/6 mice were fed normal chow diet (ND) were injected via the tail vein with control adenovirus (ctrl) or adenovirus expressing miR-802-5p one week before sacrifice. (D) Experimental scheme (left) and hepatic miR-802 levels (right) ( $n = 5$  mice). (E) Protein levels of the indicated proteins in liver lysates from 3 mice determined by IB (left) and bands quantitated using Image J (right). (F) H&E and Oil Red O staining of liver sections (left) and hepatic TG levels (right) ( $n = 4$  mice). (C, F) Scale bar (50  $\mu\text{m}$ ). (A,C,D,F) The mean and SEM are plotted and statistical significance was determined by the Student's *t*-test ( $n = 5–6$ ). *P* values are indicated.

and in reduced protein levels of AMPK $\beta$ 1 and the active form of AMPK $\alpha$ 1, phosphorylated AMPK $\alpha$ 1 (Figure 4E). SIRT1 is an upstream activator of AMPK via a LKB1-AMPK axis [39] and decreases hepatic lipid levels [40]. Overexpression of miR-802 decreased protein levels of SIRT1, which was associated with modestly increased liver TG levels (Figure 4E,F). These results suggest that overexpression of miR-802, even in lean mice, reduced expression of AMPK $\beta$ 1 and SIRT1, which contribute to decreased AMPK activity and increased liver TGs.

### 3.8. In diet-induced NASH mice, OCA-mediated beneficial effects on hepatic AMPK activity and steatosis are reversed by miR-802

Obeticholic acid (OCA), a specific agonist for the nuclear receptor FXR, is being actively tested for treatment of NASH patients [41], but

the underlying mechanisms for the OCA-mediated metabolic effects are not fully understood. Recently, we showed that defective FXR-SHP regulation in obesity aberrantly increases *miR-802* expression, promoting fatty liver, and conversely that activation of FXR by OCA reduces miR-802 levels in obese mice [15]. Since miR-802 inhibits the expression and activity of AMPK (Figures 2-4), we hypothesized that OCA-mediated beneficial effects are mediated in part by reducing miR-802 levels resulting subsequently in increased AMPK activity and improved NASH pathologies. To test this idea, we examined the effects of overexpression of miR-802 on hepatic AMPK activity and steatosis in OCA-treated mice. Mice fed a NASH-promoting high fat/cholesterol/fructose (HFHF) diet were injected with Ad-miR-802 or control virus, and then, treated daily with OCA for

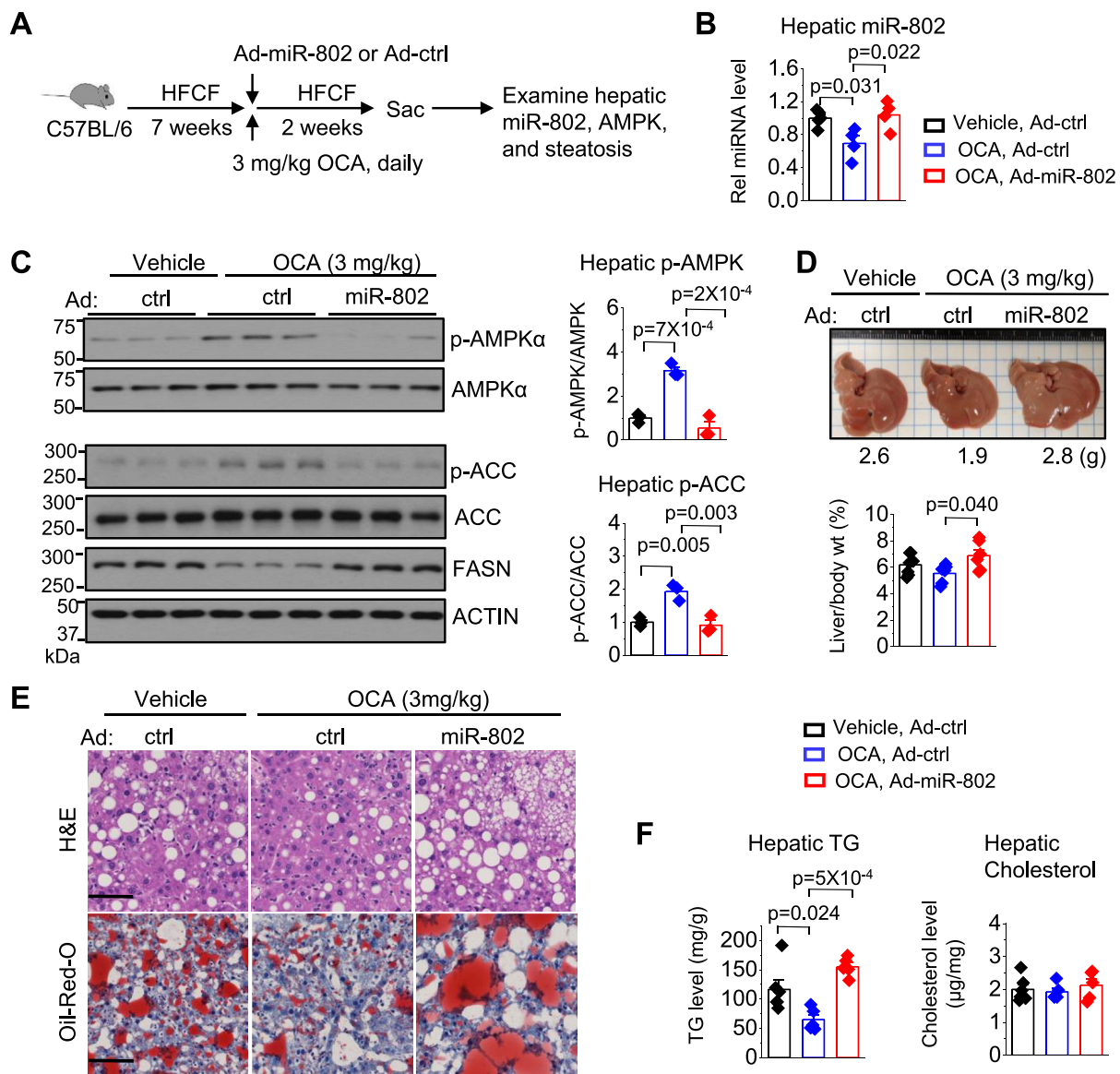


**Figure 5: In mice fed a NASH diet, OCA-mediated beneficial effects on hepatic AMPK activity and steatosis are reversed by miR-802.** C57BL/6 mice were fed a HFHF diet for 7 weeks, and then, injected via the tail vein with control adenovirus or adenovirus expressing miR-802-5p, and treated daily with a low dose of OCA (3 mg/kg mice) or vehicle for 2 weeks before sacrifice. (A) Experimental scheme. (B) Hepatic levels of miR-802 (right, n = 4 mice). (C) Levels of the indicated proteins in liver lysates determined by IB and quantitation using Image J (right, n = 3 mice). (D) Images of representative livers (top) and the ratio of liver/body weight (bottom). (E) H&E and Oil Red O staining of liver sections. Scale bar (50  $\mu$ m). (F) Liver TG and cholesterol levels. (n = 5–6 mice). (B,C,D,F) The mean and SEM are plotted. Statistical significance was determined by the one-way ANOVA. p values are indicated. NS, not significant.



2 weeks (Figure 5A). Since OCA has known side effects, such as pruritus and poor serum lipid profiles [41], we treated the mice with a much lower dose of OCA (3 mg/kg) compared to the doses utilized in published studies (10–50 mg/kg).

OCA treatment reduced hepatic levels of miR-802 and infection with Ad-miR-802 reversed the reduction (Figure 5B). Treatment with OCA increased protein levels of p-AMPK phosphorylated at Thr-172, a marker of AMPK activity [17,18,22] (Figure 5C). AMPK reduces hepatic lipid contents by inhibiting acetyl coA carboxylase (ACC) via phosphorylation at Ser-79 [42]. Consistent with increased p-AMPK, protein levels of p-ACC were increased, and those of FASN, a key lipogenic protein, were also reduced (Figure 5C). The liver size (Figure 5D), neutral lipid levels (Figure 5E), and liver TG levels (Figure 5F) were reduced in OCA-treated mice. All these OCA-mediated effects were reversed by miR-802 (Figure 5B–F).

AMPK also phosphorylates and inhibits HMG-CoA reductase (HMGCR), a key cholesterol synthetic enzyme [30]. OCA treatment substantially increased p-HMGCR levels (Supplemental Fig. 1) but did not reduce hepatic cholesterol levels (Figure 5F) possibly because of compensating actions through other regulatory pathways affecting liver cholesterol levels. Collectively, these results suggest that OCA treatment reduced miR-802 levels, which contributes to improved AMPK activity and hepatic steatosis in NASH mice.

### 3.9. OCA-mediated beneficial effects on NASH are reversed by miR-802

We next determined if the reversal by miR-802 of the OCA-mediated beneficial effects on AMPK activity and steatosis are extended to NASH pathologies, including hepatic inflammation and fibrosis. Since AMPK inhibits pro-apoptotic caspase-6 in NASH mice [26,43], we also examined the role of the miR-802-AMPK axis in hepatocyte apoptosis.

Treatment with OCA (Figure 6A) substantially reduced the number of apoptotic cells determined by TUNEL staining and reduced macrophage infiltration (Figure 6B). However, hepatic fibrosis, determined by collagen staining, was modest and detected only around hepatic portal veins, which may be due to relatively short time of feeding the NASH diet. However, OCA treatment substantially decreased fibrosis. Most of these beneficial OCA effects were reversed by miR-802 (Figure 6B,C). Overexpression of miR-802 also reversed the OCA-mediated decreases in the plasma levels of ALP and ALT, indicators of liver damage (Figure 6C).

In gene expression studies, mRNA levels of key genes involved in hepatic fibrosis, inflammation, and apoptosis, such as *Col1a1*, *Acta2*, *Tnfa*, *Cxcl1*, *Gadd45*, and *Casp6*, were reduced in OCA-treated mice, and these OCA effects were largely reversed after overexpression of miR-802 (Figure 6D). IB analyses revealed that protein levels of COL1A1, a key pro-fibrotic protein, and those of phosphorylated p65 (p-p65), a subunit of the NFκB complex, were decreased after OCA treatment (Figure 6E). Protein levels of phosphorylated JNK (p-JNK), a marker of liver damage and apoptosis, were also reduced. Remarkably, miR-802 overexpression reversed the effects of OCA on protein levels of COL1A1, p-p65, and p-JNK (Figure 6E).

Since OCA treatment increased AMPK activity (Figure 5C) and decreased apoptosis (Figure 6B), we further tested whether OCA represses caspase-6, a direct target of AMPK involved in hepatocellular apoptosis [26]. Protein levels of the active cleaved form of caspase-6 were reduced by OCA and the reduction was reversed by miR-802 (Figure 6F). These results indicate that OCA treatment increases AMPK activity and reduces NASH pathologies, particularly apoptosis, and that these beneficial OCA effects are reversed by miR-802.

### 3.10. OCA-mediated beneficial effects on NASH pathologies, particularly reduced hepatocyte apoptosis, are reversed by downregulation of AMPK

To further evaluate the role of a miR-802-AMPK axis in NASH, we tested whether the OCA-mediated beneficial effects are diminished by downregulation of AMPK (Figure 7, Supplemental Fig. 2). OCA treatment reduced the number of apoptotic cells determined by TUNEL staining and decreased hepatocyte ballooning, and hepatic inflammation determined by H&E and F4/80 staining, respectively, and these beneficial OCA effects were largely abolished by downregulation of AMPKα1 (Figure 7C). OCA treatment reduced liver fibrosis, but this OCA effect was not markedly altered by AMPK downregulation (Figure 7C). OCA treatment reduced plasma ALP and ALT levels, and these effects were blunted in AMPKα-downregulated mice (Figure 7D).

Hepatic mRNA levels of *Col1a1*, *Acta2*, *Tnfa*, *Cxcl1*, *Gadd45*, and *Casp6* were decreased after OCA treatment, but these effects were generally partially reversed by AMPKα1 downregulation (Figure 7E). OCA reduced protein levels of COL1A1, TNFα, and the cleaved form of caspase-6 and downregulation of AMPKα1 increased protein levels of both TNFα and the cleaved caspase-6 in OCA-treated mice (Figure 7F). Collectively, these results indicate that OCA reduces hepatic inflammation and apoptosis in NASH mice, and that most of these beneficial effects, particularly on reducing apoptosis, are impacted by both miR-802 and AMPK.

## 4. DISCUSSION

NAFLD is a leading cause of liver failure and death. Despite the striking global increase in NAFLD, the precise mechanisms for its pathogenesis are poorly understood. In this study, we show that obesity-induced elevated *miR-802*, in part due to defective FXR-SHP regulation [15] and activated NF-κB function [14], directly targets AMPKβ1 and reduces AMPK activity, promoting NAFLD. In addition, miR-802 in obesity may inhibit AMPK and promote NAFLD by directly or indirectly inhibiting other potential targets, such as RORα and SIRT1 (model in Figure 8). MiR-802, thus, together with obesity-associated aberrant factors and signaling, represses AMPK function to promote NAFLD/NASH.

A role for obesity-induced miR-802 in impaired glucose regulation and insulin production has been demonstrated [10,11]. We now show that miR-802 also has an important role in NAFLD/NASH. Our studies indicate that miR-802 directly binds to the 3'UTRs of both human *AMPKα1* and mouse *Ampkβ1*, leading to decreased expression and activity of AMPK, thereby, promoting NAFLD/NASH. A recent study showed that infection of mice with *S. japonicum* decreased miR-802 and increased AMPK levels, reducing hepatic lipogenesis [14]. Although NASH pathologies were not examined, this miR-802-parasite study is largely consistent with our finding that obesity-induced miR-802 reduces AMPK expression/activity, thereby promoting fatty liver. The *Ampkα1* subunit was also inhibited by miR-291, facilitating lipogenesis [44]. Recently, Song and colleague demonstrated that miR-378 promotes hepatic inflammation and fibrosis in NASH via silencing of the *AMPKγ2* subunit and subsequently, activation of the NFκB-TNFα [45]. Thus, our findings, together with published miR studies [38,44,45], indicate that all three subunits of AMPK are inhibited by multiple miRs in NAFLD.

Expression of miR-802 is elevated in obese and NAFLD patients and also in the liver, kidney, islets, and serum of obese mice [10,11,14,15]. Recent studies showed that nuclear levels of FOXO1 are substantially increased, leading to upregulation of *miR-802* in the islets of obese

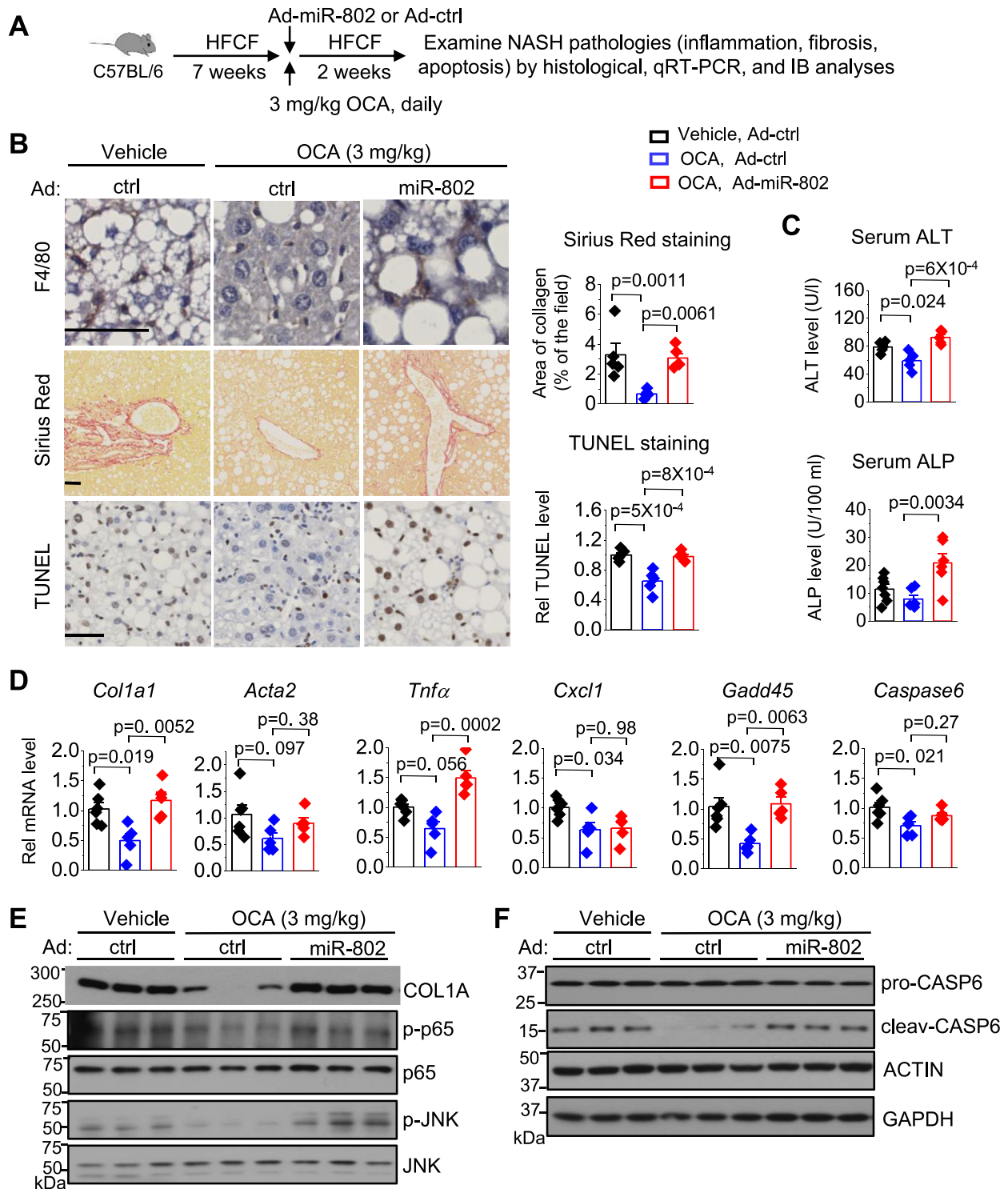


**Figure 6: OCA-mediated beneficial therapeutic effects on NASH pathologies, including inflammation, fibrosis, and apoptosis, are reversed by miR-802.** C57BL/6 mice were fed and treated as described in Figure 5. (A) Experimental scheme. (B) Liver sections stained with F4/80, Sirius Red, and TUNEL for detection of hepatic inflammation, fibrosis (collagen), and apoptosis, respectively (left). Scale bar (50  $\mu$ m). Image analyses were done using Image J and the area of collagen staining and TUNEL levels were quantified (right,  $n = 5$  mice). (C) Plasma ALT and ALP levels. (D) mRNA levels of indicated genes ( $n = 5-6$  mice). (E, F) Levels of the indicated proteins determined by IB (left,  $n = 3$  mice). (B-D) The mean and SEM are plotted and statistical significance was determined by the one-way ANOVA.  $p$  values are indicated. NS, not significant.

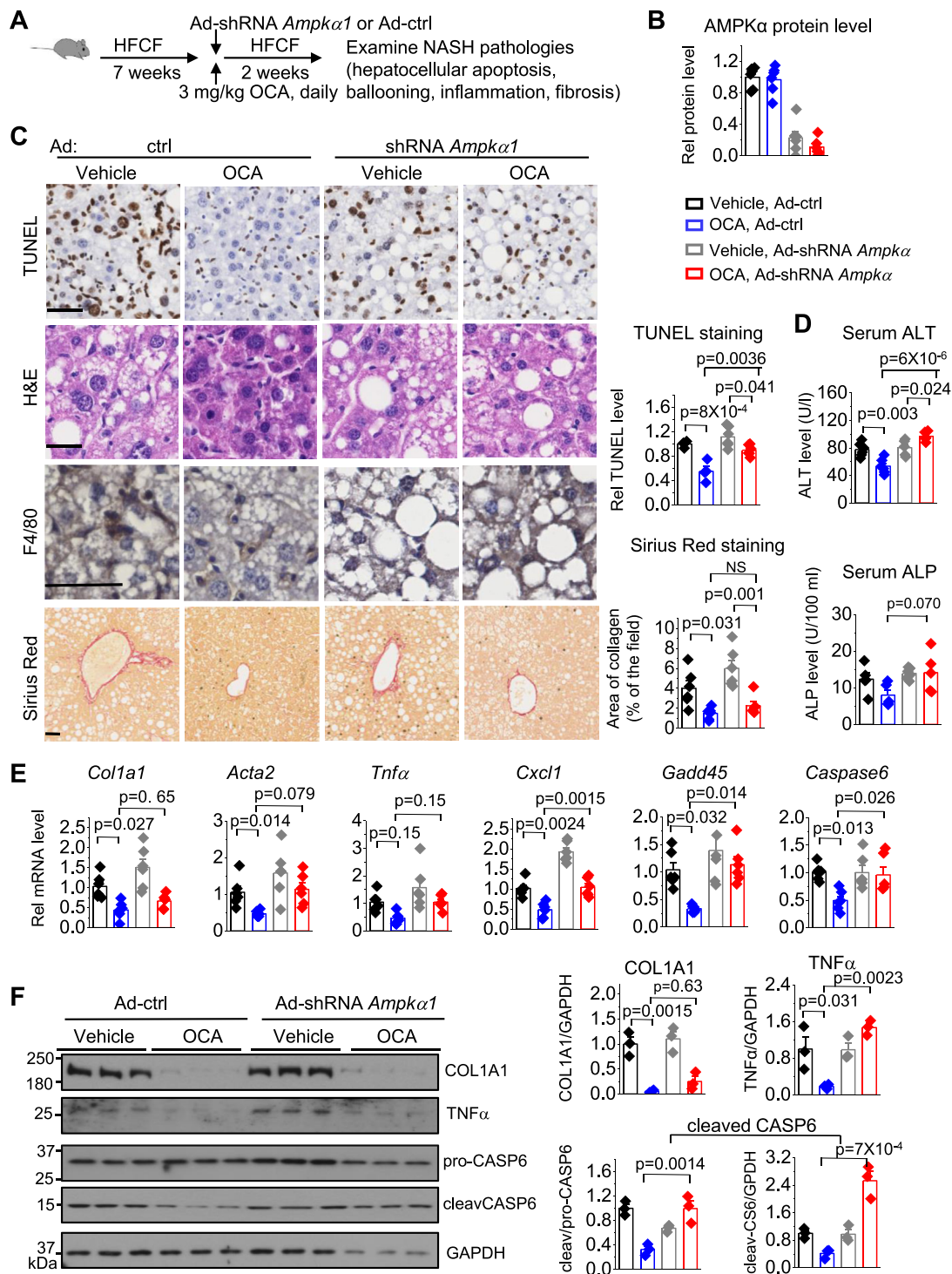


**Figure 7: OCA-mediated beneficial effects on NASH pathologies, particularly reducing apoptosis, are reversed by downregulation of AMPK.** Mice were fed a NASH diet for 7 weeks and injected via tail veins with adenovirus expressing shRNA of *Ampkα1* or control GFP, and 2 weeks later, the mice were sacrificed. (A) Experimental scheme. (B) Quantitation of protein levels of AMPK $\alpha$  detected by IB using Image J ( $n = 3$  mice). (C) Liver sections stained with TUNEL, H&E, F4/80, and Sirius Red for detection of hepatocyte apoptosis, ballooning, inflammation, and fibrosis (collagen), respectively (left). Scale bar (50  $\mu$ m). Image analyses were done using Image J and the area of TUNEL and collagen levels were quantified (right,  $n = 4-6$  mice). (D) Plasma ALT and ALP levels. (E) mRNA levels of indicated genes ( $n = 5-6$  mice). (F) Levels of the indicated proteins determined by IB ( $n = 3$  mice, left) and quantitation using Image J (right). (B-F) The mean and SEM are plotted and statistical significance was determined by the one-way ANOVA.  $p$  values are indicated. NS, not significant.



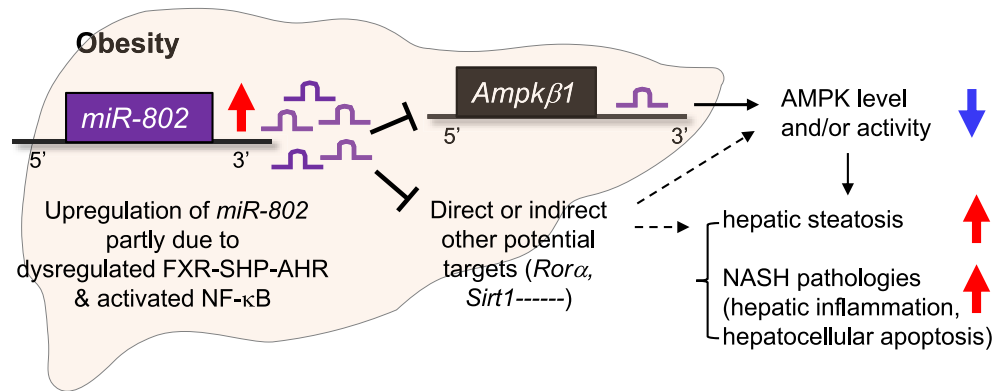


**Figure 8: A new role of a miR-802-AMPK axis in promoting NAFLD/NASH. Model:** Hepatic expression of *miR-802* is aberrantly increased in obesity in part due to defective FXR-SHP repression of AHR, an activator of *miR-802*, and activated NF-κB function. Obesity-induced *miR-802* inhibits hepatic AMPK by binding to the 3'UTR of *Ampkβ1* mRNA, promoting hepatic steatosis and NASH pathologies, including hepatic inflammation and hepatocellular apoptosis in mice. Obesity-induced *miR-802* also inhibits AMPK and promotes NAFLD/NASH by directly or indirectly inhibiting other potential targets, such as *RORα* and *SIRT1*. OCA-mediated beneficial effects on NASH pathologies, particularly hepatocellular apoptosis, are reversed by overexpression of *miR-802* or downregulation of AMPK. The *miR-802*-AMPK axis may, thus, represent new therapeutic targets for the treatment of NAFLD/NASH.

mice [11]. Furthermore, a dysregulated FXR-SHP-AHR axis in obesity increased transcription of *miR-802* in the liver [15]. Activated NF-κB also increased hepatic expression of *miR-802* [14]. Indeed, the promoter region of *miR-802* contains multiple binding sites for NF-κB and STATs (Supplemental Fig. 3). Thus, transcription of *miR-802* is likely elevated in obesity and NAFLD by dysregulated transcriptional factors and inflammatory signaling.

Numerous previous studies have revealed the promising therapeutic potential of OCA in liver disease [16,41]. OCA protected against cholestatic liver damage by reducing hepatic inflammation and fibrosis in mice [46]. OCA also inhibited liver cell death by suppressing metabolic stress-induced p53 activation in NASH mice [47]. In the present study, OCA activation of FXR improved AMPK activity and reduced expression of hepatic genes promoting NASH pathologies, and most of the OCA-mediated beneficial effects were reversed by *miR-802* overexpression or AMPK downregulation. FXR also regulates numerous genes in the intestine, including the gut hormone FGF15/19, to maintain healthy lipid levels by inhibiting bile acid/lipid synthesis, intestinal lipid absorption and bile acid recycling [32,48,49]. Thus, OCA activation of FXR leads to amelioration of NASH by directly acting on hepatic FXR-SHP-*miR-802* pathway but also indirectly through the gut-liver crosstalk.

The gene-regulatory function of FXR can be modulated in physiology and disease by post-translational modifications [31,36,50,51]. Relevant to our present study, a previous study showed that AMPK phosphorylates FXR and inhibits its transcriptional activity in a gene-selective manner, promoting liver injury under cholestatic conditions [31]. Consistent with this previous study, OCA treatment increased AMPK activity and substantially increased p-FXR levels in NASH mice (Supplemental Fig. 4), leading to differential regulation of direct FXR targets involved in hepatic metabolism, including *Shp*, *Bsep*, *Scarb1*, *βKL*, and *Atg7*, and an indirect target, *Cyp7a1* (Supplemental Fig. 5). Although OCA-induced AMPK may inhibit FXR activity via phosphorylation, it is likely that this inhibition only partially counteracts the direct activation of FXR by OCA since OCA activation of FXR had overall beneficial effects on NASH.

Recently, Zhao et al. demonstrated that an AMPK-caspase-6 axis is a key regulator of liver damage and apoptosis in NASH mice [26]. Consistent with this study, OCA activation of FXR improved AMPK

activity, resulting in decreased active caspase-6 levels and reduced apoptosis in NASH mice. FXR maintains healthy liver and homeostasis by transcriptional repression of inflammation, autophagy, and apoptosis [46,50,52]. The published FXR ChIP-seq data in dietary obese mice [53] revealed that treatment with GW4064, an FXR agonist, increased FXR binding peaks within the *caspase-6* gene (Supplemental Fig. 6). These genomic data, together with OCA-mediated decreased mRNA levels of *caspase-6*, imply that activation of FXR may inhibit hepatocyte apoptosis via direct repression of *Caspase-6*, in addition to repression of *miR-802* [15]. Future research will be needed to test whether FXR protects against liver damage by transcriptional repression of pro-apoptotic genes.

A recent study demonstrated that while reactivation of AMPK in NAFLD improved hepatic steatosis, complete liver-specific knockout of AMPK did not promote fatty liver development [25]. In the present study, overexpression of *miR-802* decreased protein levels of AMPKβ1 and reduced AMPK activity, which was associated with modestly increased hepatic TGs. Although these conflicting results may be due to different experimental conditions, *miR-802* may promote fatty liver and NASH pathologies by inhibiting additional targets, including *RORα*, which contain a binding site for *miR-802* (Supplemental Fig. 7). *RORα* was shown to activate AMPK, attenuating fatty liver [54]. Indeed, the 3'UTR of *Rorα* contains a binding site for *miR-802* (Supplemental Fig. 7A) and overexpression of *miR-802* reduced protein levels of *RORα* in both lean and dietary obese mice (Supplemental Figs. 8 and 9). MiRs often negatively regulate multiple targets in the same disease processes [4–9]. Obesity-induced *miR-802*, may, thus, inhibit AMPK activity and promote fatty liver, not only by directly targeting AMPKβ1, but also by directly or indirectly inhibiting other potential targets, such as *RORα* and *SIRT1*.

In summary, we present evidence demonstrating a functional link between elevated *miR-802* levels in obesity and impaired AMPK function, which promotes NAFLD/NASH. We further show that overexpression of *miR-802* or downregulation of AMPK reversed most of the beneficial therapeutic effects of OCA on NASH pathologies, particularly the reduction of hepatocellular apoptosis. As both *miR-802* and AMPK are highly conserved in humans and mice, the *miR-802*-AMPK axis identified in this study may represent a novel therapeutic target for the treatment of NAFLD/NASH patients.



## CONTRIBUTIONS

HS and JK designed research; HS, SS, and HJ performed experiments; HS, SS, HJ, and BK analyzed data; and HS, BK, and JK wrote the paper.

## FINANCIAL SUPPORT

This study was supported by grants from the National Institutes of Health (DK062777 and DK095842) to JKK.

## DATA AVAILABILITY

Data will be made available on request.

## ACKNOWLEDGMENTS

We thank the Liver Tissue Cell Distribution System, University of Minnesota (NIH Contract # HHSN276201200017C), for providing liver specimens of NAFLD steatosis patients and individuals without liver disease. We also thank Dr. Jinjing Chen for her help and expertise with the NASH mouse studies. This study was supported by grants from the National Institutes of Health (DK062777 and DK095842) to JKK.

## CONFLICT OF INTEREST

The authors declare no conflict of interest.

## APPENDIX A. SUPPLEMENTARY DATA

Supplementary data to this article can be found online at <https://doi.org/10.1016/j.molmet.2022.101603>.

## REFERENCES

- [1] Friedman, S.L., Neuschwander-Tetri, B.A., Rinella, M., Sanyal, A.J., 2018. Mechanisms of NAFLD development and therapeutic strategies. *Nature Medicine* 24(7):908–922.
- [2] Loomba, R., Friedman, S.L., Shulman, G.I., 2021. Mechanisms and disease consequences of nonalcoholic fatty liver disease. *Cell* 184(10):2537–2564.
- [3] Gjorgjieva, M., Sobolewski, C., Dolicka, D., Correia de Sousa, M., Foti, M., 2019. miRNAs and NAFLD: from pathophysiology to therapy. *Gut* 68(11):2065–2079.
- [4] Lee, J., Padhye, A., Sharma, A., Song, G., Miao, J., Mo, Y.Y., et al., 2010. A pathway involving farnesoid X receptor and small heterodimer partner positively regulates hepatic sirtuin 1 levels via microRNA-34a inhibition. *Journal of Biological Chemistry* 285(17):12604–12611.
- [5] Fu, T., Choi, S.E., Kim, D.H., Seok, S., Suino-Powell, K.M., Xu, H.E., et al., 2012. Aberrantly elevated microRNA-34a in obesity attenuates hepatic responses to FGF19 by targeting a membrane coreceptor beta-Klotho. *Proceedings of the National Academy of Sciences of the United States of America* 109:16137–16142.
- [6] Choi, S.E., Fu, T., Seok, S., Kim, D.H., Yu, E., Lee, K.W., et al., 2013. Elevated microRNA-34a in obesity reduces NAD levels and SIRT1 activity by directly targeting NAMPT. *Aging Cell* 12:1062–1072.
- [7] Xu, Y., Zalzal, M., Xu, J., Li, Y., Yin, L., Zhang, Y., 2015. A metabolic stress-inducible miR-34a-HNF4alpha pathway regulates lipid and lipoprotein metabolism. *Nature Communications* 6:7466.
- [8] Ding, J., Li, M., Wan, X., Jin, X., Chen, S., Yu, C., et al., 2015. Effect of miR-34a in regulating steatosis by targeting PPARalpha expression in nonalcoholic fatty liver disease. *Scientific Reports* 5:13729.
- [9] Xu, Y., Zhu, Y., Hu, S., Pan, X., Bawa, F.C., Wang, H.H., et al., 2021. Hepatocyte miR-34a is a key regulator in the development and progression of non-alcoholic fatty liver disease. *Molecular Metabolism* 51:101244.
- [10] Kornfeld, J.W., Baitzel, C., Konner, A.C., Nicholls, H.T., Vogt, M.C., Herrmanns, K., et al., 2013. Obesity-induced overexpression of miR-802 impairs glucose metabolism through silencing of Hnf1b. *Nature* 494(7435):111–115.
- [11] Zhang, F., Ma, D., Zhao, W., Wang, D., Liu, T., Liu, Y., et al., 2020. Obesity-induced overexpression of miR-802 impairs insulin transcription and secretion. *Nature Communications* 11(1):1822.
- [12] Han, H.S., Choi, B.H., Kim, J.S., Kang, G., Koo, S.H., 2017. Hepatic Crtc2 controls whole body energy metabolism via a miR-34a-Fgf21 axis. *Nature Communications* 8(1):1878.
- [13] Han, H.S., Kim, S.G., Kim, Y.S., Jang, S.H., Kwon, Y., Choi, D., et al., 2022. A novel role of CRTC2 in promoting nonalcoholic fatty liver disease. *Molecular Metabolism* 55:101402.
- [14] Ni, Y., Xu, Z., Li, C., Zhu, Y., Liu, R., Zhang, F., et al., 2021. Therapeutic inhibition of miR-802 protects against obesity through AMPK-mediated regulation of hepatic lipid metabolism. *Theranostics* 11(3):1079–1099.
- [15] Seok, S., Sun, H., Kim, Y.C., Kemper, B., Kemper, J.K., 2021. Defective FXR-SHP regulation in obesity aberrantly increases miR-802 expression, promoting insulin resistance and fatty liver. *Diabetes* 70(3):733–744.
- [16] Abenavoli, L., Falalyeyeva, T., Boccutto, L., Tsyryuk, O., Kobyljak, N., 2018. Obeticholic acid: a new era in the treatment of nonalcoholic fatty liver disease. *Pharmaceuticals* 11(4).
- [17] Steinberg, G.R., Kemp, B.E., 2009. AMPK in health and disease. *Physiological Reviews* 89(3):1025–1078.
- [18] Herzig, S., Shaw, R.J., 2018. AMPK: guardian of metabolism and mitochondrial homeostasis. *Nature Reviews Molecular Cell Biology* 19(2):121–135.
- [19] Viollet, B., Horman, S., Leclerc, J., Lantier, L., Foretz, M., Billaud, M., et al., 2010. AMPK inhibition in health and disease. *Critical Reviews in Biochemistry and Molecular Biology* 45(4):276–295.
- [20] Woods, A., Williams, J.R., Muckett, P.J., Mayer, F.V., Lijevald, M., Bohlooly, Y.M., et al., 2017. Liver-specific activation of AMPK prevents steatosis on a high-fructose diet. *Cell Reports* 18(13):3043–3051.
- [21] Garcia, D., Hellberg, K., Chaix, A., Wallace, M., Herzig, S., Badur, M.G., et al., 2019. Genetic liver-specific AMPK activation protects against diet-induced obesity and NAFLD. *Cell Reports* 26(1):192–208 e196.
- [22] Jeon, S.M., 2016. Regulation and function of AMPK in physiology and diseases. *Experimental and Molecular Medicine* 48(7):e245.
- [23] Smith, B.K., Marcinko, K., Desjardins, E.M., Lally, J.S., Ford, R.J., Steinberg, G.R., 2016. Treatment of nonalcoholic fatty liver disease: role of AMPK. *American Journal of Physiology - Endocrinology And Metabolism* 311(4):E730–E740.
- [24] Gluais-Dagorn, P., Foretz, M., Steinberg, G.R., Batchuluun, B., Zawistowska-Deniziak, A., Lambooji, J.M., et al., 2022. Direct AMPK activation corrects NASH in rodents through metabolic effects and direct action on inflammation and fibrogenesis. *Hepatology* 75(1):101–119.
- [25] Boudaba, N., Marion, A., Huet, C., Pierre, R., Viollet, B., Foretz, M., 2018. AMPK Re-activation suppresses hepatic steatosis but its downregulation does not promote fatty liver development. *EBioMedicine* 28:194–209.
- [26] Zhao, P., Sun, X., Chagga, C., Liao, Z., In Wong, K., He, F., et al., 2020. An AMPK-caspase-6 axis controls liver damage in nonalcoholic steatohepatitis. *Science* 367(6478):652–660.
- [27] Kim, D.H., Kwon, S., Byun, S., Xiao, Z., Park, S., Wu, S.Y., et al., 2016. Critical role of RanBP2-mediated SUMOylation of Small Heterodimer Partner in maintaining bile acid homeostasis. *Nature Communications* 7:12179.
- [28] Kim, D.H., Kwon, S., Byun, S., Xiao, Z., Park, S., Wu, S.Y., et al., 2016. Critical role of RanBP2-mediated SUMOylation of Small Heterodimer Partner in maintaining bile acid homeostasis. *Nature Communications* 7:12179.

- [29] Kim, Y.C., Seok, S., Byun, S., Kong, B., Zhang, Y., Guo, G., et al., 2018. AhR and SHP regulate phosphatidylcholine and S-adenosylmethionine levels in the one-carbon cycle. *Nature Communications* 9(1):540.
- [30] Loh, K., Tam, S., Murray-Segal, L., Huynh, K., Meikle, P.J., Scott, J.W., et al., 2019. Inhibition of adenosine monophosphate-activated protein kinase-3-hydroxy-3-methylglutaryl coenzyme A reductase signaling leads to hypercholesterolemia and promotes hepatic steatosis and insulin resistance. *Hepatology* 69(3):84–98.
- [31] Lien, F., Berthier, A., Bouchaert, E., Gheeraert, C., Alexandre, J., Porez, G., et al., 2014. Metformin interferes with bile acid homeostasis through AMPK-FXR crosstalk. *The Journal of Clinical Investigation* 124(3):1037–1051.
- [32] Kim, Y., Seok, S., Zhang, Y., Ma, J., Kong, B., Guo, G., et al., 2020. Intestinal FGF15/19 physiologically repress hepatic lipogenesis in the late fed-state by activating SHP and DNMT3A. *Nature Communications* 11:5969.
- [33] Byun, S., Seok, S., Kim, Y.C., Zhang, Y., Yau, P., Iwamori, N., et al., 2020. Fasting-induced FGF21 signaling activates hepatic autophagy and lipid degradation via JMJD3 histone demethylase. *Nature Communications* 11(1):807.
- [34] Seok, S., Kim, Y.C., Byun, S., Choi, S., Xiao, Z., Iwamori, N., et al., 2018. Fasting-induced JMJD3 histone demethylase epigenetically activates mitochondrial fatty acid beta-oxidation. *Journal of Clinical Investigation* 128(7):3144–3159.
- [35] Miao, J., Xiao, Z., Kanamaluru, D., Min, G., Yau, P.M., Veenstra, T.D., et al., 2009. Bile acid signaling pathways increase stability of Small Heterodimer Partner (SHP) by inhibiting ubiquitin-proteasomal degradation. *Genes & Development* 23(8):986–996.
- [36] Kemper, J.K., Xiao, Z., Ponugoti, B., Miao, J., Fang, S., Kanamaluru, D., et al., 2009. FXR acetylation is normally dynamically regulated by p300 and SIRT1 but constitutively elevated in metabolic disease states. *Cell Metabolism* 10(5):392–404.
- [37] Kwon, S., Seok, S., Yau, P., Li, X., Kemper, B., Kemper, J.K., 2017. Obesity and aging diminish sirtuin 1 (SIRT1)-mediated deacetylation of SIRT3, leading to hyperacetylation and decreased activity and stability of SIRT3. *Journal of Biological Chemistry* 292(42):17312–17323.
- [38] Zhang, C., Seo, J., Murakami, K., Salem, E.S.B., Bernhard, E., Borra, V.J., et al., 2018. Hepatic Ago2-mediated RNA silencing controls energy metabolism linked to AMPK activation and obesity-associated pathophysiology. *Nature Communications* 9(1):3658.
- [39] Canto, C., Auwerx, J., 2009. PGC-1alpha, SIRT1 and AMPK, an energy sensing network that controls energy expenditure. *Current Opinion in Lipidology* 20(2):98–105.
- [40] Ponugoti, B., Kim, D.H., Xiao, Z., Smith, Z., Miao, J., Zang, M., et al., 2010. SIRT1 deacetylates and inhibits SREBP-1C activity in regulation of hepatic lipid metabolism. *Journal of Biological Chemistry* 285(44):33959–33970.
- [41] Ali, A.H., Carey, E.J., Lindor, K.D., 2015. Recent advances in the development of farnesoid X receptor agonists. *Annals of Translational Medicine* 3(1):5.
- [42] Lally, J.S.V., Ghoshal, S., DePeralta, D.K., Moaven, O., Wei, L., Masia, R., et al., 2019. Inhibition of acetyl-CoA carboxylase by phosphorylation or the inhibitor ND-654 suppresses lipogenesis and hepatocellular carcinoma. *Cell Metabolism* 29(1):174–182 e175.
- [43] Zhao, P., Saltiel, A.R., 2020. From overnutrition to liver injury: AMP-activated protein kinase in nonalcoholic fatty liver diseases. *Journal of Biological Chemistry* 295(34):12279–12289.
- [44] Meng, X., Guo, J., Fang, W., Dou, L., Li, M., Huang, X., et al., 2016. Liver MicroRNA-291b-3p promotes hepatic lipogenesis through negative regulation of adenosine 5'-monophosphate (AMP)-activated protein kinase alpha1. *Journal of Biological Chemistry* 291(20):10625–10634.
- [45] Zhang, T., Hu, J., Wang, X., Zhao, X., Li, Z., Niu, J., et al., 2019. MicroRNA-378 promotes hepatic inflammation and fibrosis via modulation of the NF-kappaB-TNFalpha pathway. *Journal of Hepatology* 70(1):87–96.
- [46] Jung, H., Chen, J., Hu, X., Sun, H., Wu, S.Y., Chiang, C.M., et al., 2020. BRD4 inhibition and FXR activation, individually beneficial in cholestasis, are antagonistic in combination. *JCI Insight* 6(1).
- [47] Goto, T., Itoh, M., Suganami, T., Kanai, S., Shirakawa, I., Sakai, T., et al., 2018. Obeticholic acid protects against hepatocyte death and liver fibrosis in a murine model of nonalcoholic steatohepatitis. *Scientific Reports* 8(1):8157.
- [48] Kim, Y.C., Byun, S., Seok, S., Guo, G., Xu, H.E., Kemper, B., et al., 2018. Small heterodimer partner and fibroblast growth factor 19 inhibit expression of NPC1L1 in mouse intestine and cholesterol absorption. *Gastroenterology* 156:1052–1065.
- [49] Byun, S., Kim, Y.C., Zhang, Y., Kong, B., Guo, G., Sadoshima, J., et al., 2017. A postprandial FGF19-SHP-LSD1 regulatory axis mediates epigenetic repression of hepatic autophagy. *EMBO Journal* 36(12):1755–1769.
- [50] Kim, D.H., Xiao, Z., Kwon, S., Sun, X., Ryerson, D., Tkac, D., et al., 2015. A dysregulated acetyl/SUMO switch of FXR promotes hepatic inflammation in obesity. *EMBO Journal* 34(2):184–199.
- [51] Byun, S., Kim, D.H., Ryerson, D., Kim, Y.C., Sun, H., Kong, B., et al., 2018. Postprandial FGF19-induced phosphorylation by Src is critical for FXR function in bile acid homeostasis. *Nature Communications* 9(1):2590.
- [52] Seok, S., Fu, T., Choi, S.E., Li, Y., Zhu, R., Kumar, S., et al., 2014. Transcriptional regulation of autophagy by an FXR-CREB axis. *Nature* 516(7529):108–111.
- [53] Lee, J., Seok, S.M., Yu, P., Kim, K., Smith, Z., Rivas-Astroza, M., et al., 2012. Genomic analysis of hepatic Farnesoid X Receptor (FXR) binding sites reveals altered binding in obesity and direct gene repression by FXR. *Hepatology* 56:108–117.
- [54] Kim, E.J., Yoon, Y.S., Hong, S., Son, H.Y., Na, T.Y., Lee, M.H., et al., 2012. Retinoic acid receptor-related orphan receptor alpha-induced activation of adenosine monophosphate-activated protein kinase results in attenuation of hepatic steatosis. *Hepatology* 55(5):1379–1388.